Channels 6:3, 166-173; May/June 2012; © 2012 Landes Bioscience

Rem-GTPase regulates cardiac myocyte L-type calcium current

Janos Magyar,[1,2,†] Carmen E. Kiper,[1,†] Gail Sievert,[1] Weikang Cai,[3] Geng-Xian Shi,[3] Shawn M. Crump,[1] Liren Li,[4] Steven Niederer,[4] Nic Smith,[4] Douglas A. Andres[3] and Jonathan Satin[1,*]

[1]Department of Physiology; University of Kentucky College of Medicine; Lexington, KY USA; [2]Department of Physiology; MHSC; University of Debrecen; Debrecen, Hungary; [3]Department of Molecular and Cellular Biochemistry; University of Kentucky College of Medicine; Lexington, KY USA; [4]Computer Laboratory; University of Oxford; Oxford, UK

[†]These authors contributed equally to this work.

Keywords: L-type calcium channel, Ras-GTPase, calcium current, patch-clamp

Abbreviations: LTCC, L-type calcium channel; Ca, Ca^{2+} or calcium ion; RGK, Rem, Rad, Rem2, Gem/Kir subfamily of Ras-related small GTPase; $I_{Ca,L}$, L-type calcium channel current; TAC, thoracic aorta constriction; CaM, calmodulin; CaMKII, calmodulin kinase II; $Rem^{-/-}$, Rem-null mouse; ECG, electrocardiogram; NCX, sodium-calcium exchange protein; PLB, phospholamban; DCT, distal carboxyl terminus of $Ca_V1.2$

Rationale: The L-type calcium channels (LTCC) are critical for maintaining Ca^{2+}-homeostasis. In heterologous expression studies, the RGK-class of Ras-related G-proteins regulates LTCC function; however, the physiological relevance of RGK-LTCC interactions is untested.

Objective: In this report we test the hypothesis that the RGK protein, Rem, modulates native Ca^{2+} current ($I_{Ca,L}$) via LTCC in murine cardiomyocytes.

Methods and Results: Rem knockout mice ($Rem^{-/-}$) were engineered, and $I_{Ca,L}$ and Ca^{2+}-handling properties were assessed. $Rem^{-/-}$ ventricular cardiomyocytes displayed increased $I_{Ca,L}$ density. $I_{Ca,L}$ activation was shifted positive on the voltage axis, and β-adrenergic stimulation normalized this shift compared with wild-type $I_{Ca,L}$. Current kinetics, steady-state inactivation and facilitation was unaffected by $Rem^{-/-}$. Cell shortening was not significantly different. Increased $I_{Ca,L}$ density in the absence of frank phenotypic differences motivated us to explore putative compensatory mechanisms. Despite the larger $I_{Ca,L}$ density, $Rem^{-/-}$ cardiomyocyte Ca^{2+} twitch transient amplitude was significantly less than that compared with wild type. Computer simulations and immunoblot analysis suggests that relative dephosphorylation of $Rem^{-/-}$ LTCC can account for the paradoxical decrease of Ca^{2+} transients.

Conclusions: This is the first demonstration that loss of an RGK protein influences $I_{Ca,L}$ in vivo in cardiac myocytes.

Introduction

L-type Ca channels (LTCC) are critical for maintaining Ca-homeostasis, providing trigger Ca for Ca-induced Ca-release, and regulating electrical function in cardiac myocytes. Therefore, precise control of LTCC function has profound implications for cardiac myocyte physiology. LTCC exist as a multi-protein complex in cardiac myocytes.[1] Thus, understanding of LTCC function requires evaluation of LTCC Ca current ($I_{Ca,L}$) in native complexes. Cardiac myocyte LTCC consists of the main pore-forming subunit in complex with accessory proteins including $Ca_V\beta2$ family members, α2δ and calmodulin (CaM; reviewed in ref. 2). In addition, we, and others have recently extensively characterized the ability of the RGK-family of monomeric G-proteins to modulate $I_{Ca,L}$.[3-6]

The RGK family of Ras-related monomeric G-proteins includes Rem, Rem2, Rad and Gem/Kir.[7] Rem and Rad are expressed in myocardium.[8,9] Rad co-expressed with recombinant LTCC show block of current,[10] and therefore, reduction of Rad in vivo is expected to increase $I_{Ca,L}$. Rad is downregulated in experimental induced heart failure (thoracic aorta constriction, TAC) in mice.[11] Rad knockout mice show no functional phenotype at baseline, but following TAC CaMKII increases.[11] Rad knockdown via RNAi results in an increase of $I_{Ca,L}$, Ca transients and contractility.[12]

Heterologous expression studies document Rem blockade of $I_{Ca,L}$;[5,10,13-15] however, there are no reports that assess in vivo Rem function. Overexpression of Rem, and other RGK proteins, results in prominent blockade of cardiac myocyte $I_{Ca,L}$.[4,16] Therefore, we tested the hypothesis that depletion of Rem results in an increase of $I_{Ca,L}$. In this report, we examined cardiac myocyte $I_{Ca,L}$ in Rem-null mice ($Rem^{-/-}$). Cardiac myocyte $I_{Ca,L}$ density increases in $Rem^{-/-}$ compared with that from wild-type mice. Nevertheless, Rem-deletion results in no frank cardiac phenotype at baseline.

*Correspondence to: Jonathan Satin; Email: jsatin1@uky.edu
Submitted: 06/08/11; Revised: 03/27/12; Accepted: 03/28/12
http://dx.doi.org/10.4161/chan.20192

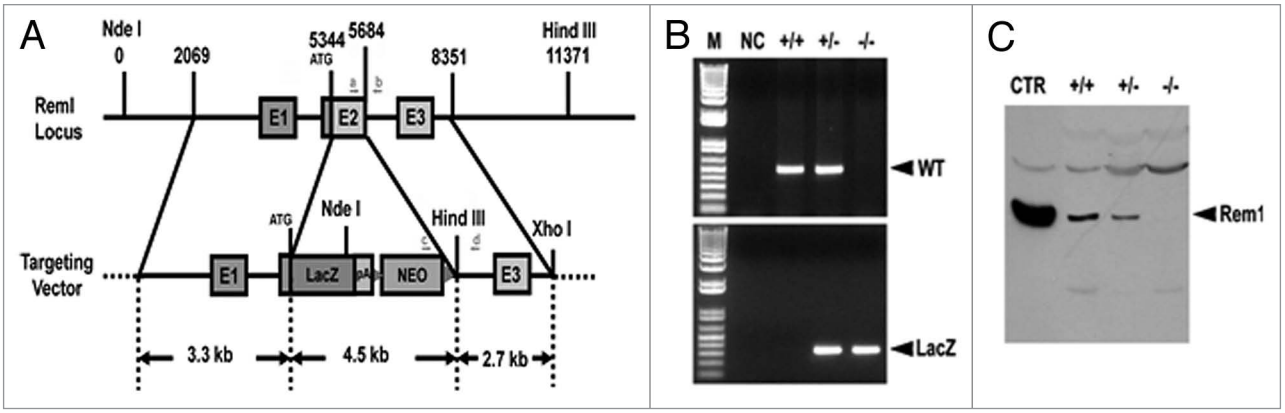

Figure 1. Rem knockout mouse. (A) Schematic representation of the strategy used to generate the Rem knockout mouse. The coding region of Exon 2 was targeted and replaced by a LacZ expressing cassette, followed by the neomycin gene flanked by FRT sites. Arrows indicate the location of genotyping primers (a–d). (B) Genomic DNA was isolated from mouse tail biopsies, and subjected to PCR analysis using the oligonucleotide primer pairs indicated in (A). A 348 base pair band represents the mutant allele (lower part; amplification using primer pair c/d), while a 500 base pair band represents the wild-type allele (upper part; amplification using primer pair a/b). (C) Total protein was isolated from hearts obtained from Rem mutant or WT-littermates, and subjected to anti-Rem immunoblot analysis. Wild-type Rem expressed in HEK293 cells was included as a positive control. Note that Rem protein levels are completely eliminated in $Rem^{-/-}$ cardiac muscle, while reduced in $Rem^{+/-}$ animals.

The increased $I_{Ca,L}$ density may be offset by a positive shift of the steady-state activation curve. Thus, our data support the notion that compensatory changes in Ca homeostasis preserve cardiac function.

Results

$I_{Ca,L}$ in $Rem^{-/-}$ cardiac myocytes. Rem overexpression blocks $I_{Ca,L}$ in heterologous expression systems,[14] and in cardiac myocytes.[16] These results suggested that Rem governs $I_{Ca,L}$ in vivo. To test this idea, we generated a Rem1 knockout mouse (**Fig. 1**). Rem null mutant mice ($Rem^{-/-}$) were born at the expected Mendelian ratio, and grew to adulthood without showing any discernible abnormalities.

To examine the contribution of Rem to LTCC function, we measured $I_{Ca,L}$ in $Rem^{-/-}$ cardiac myocytes. The expectation is that $I_{Ca,L}$ should increase in the absence of Rem blockade of current. As the analog traces of **Figure 2A** shows the $I_{Ca,L}$ density was significantly greater in $Rem^{-/-}$ compared with age-matched wild-type controls (peak $I_{Ca,L}$ density amplitudes at +10 mV: -19.0 ± 0.5 pA/pF (n = 55) for $Rem^{-/-}$ and -16.0 ± 1.0 pA/pF (n = 40) for the age-matched wild-type controls; $p < 0.05$). The current-voltage relationships [I(V)] show that the differences in calcium current densities were statistically significant in the membrane potential range between 0 mV and +45 mV (**Fig. 2B**). These data are consistent with Rem governing $I_{Ca,L}$ amplitude in cardiomyocytes.

The maximal $I_{Ca,L}$ was greater in $Rem^{-/-}$ compared with wild-type control, and examination of the I(V) curves reveals a shift in the voltage dependence of $I_{Ca,L}$ (**Fig. 2B**). **Figure 2C** shows that the midpoint of activation of $Rem^{-/-}$ $I_{Ca,L}$ is significantly shifted relative to control myocytes (-7.2 ± 0.3 mV and -3.3 ± 0.2 mV at wild-type and $Rem^{-/-}$ myocytes respectively, $p < 0.05$). The voltage dependence of steady-state inactivation was measured by a double pulse protocol. As **Figure 2C** demonstrates Rem deletion does not affect the voltage dependence of steady-state inactivation. Thus the theoretical steady-state window Ca-current was reduced in $Rem^{-/-}$ cardiac myocytes (**Fig. 2C** and shaded area). Taken together, there is an increase of maximal-activated $I_{Ca,L}$ that is potentially compensated by a shift of steady-state activation.

$I_{Ca,L}$ kinetics are key determinants of total Ca^{2+}-entry into the cytosol, and in heterologous expression systems Rem alteration of kinetics depends on exogenous CaM expression.[5] To evaluate whether Rem alters native $I_{Ca,L}$ we measured $I_{Ca,L}$ kinetics in cardiomyocytes. $I_{Ca,L}$ kinetics were unaffected by $Rem^{-/-}$. The effect of Rem on the time dependent inactivation of $I_{Ca,L}$ was determined by bi-exponential fitting to the decay of current. The tau_1 values were 24.7 ± 2.2 ms and 25.5 ± 1.8 ms for wild type and $Rem^{-/-}$, respectively. The tau_2 values were 5.0 ± 0.8 ms and 5.3 ± 0.6 ms (**Fig. S1**). As expected, the fast and slow component amplitudes of $Rem^{-/-}$ were significantly larger than that of the age-matched wild-type controls ($p < 0.05$) but the relative amplitudes of the fast/slow components were not different between $Rem^{-/-}$ and control. The effect of Rem was also tested on the facilitation of $I_{Ca,L}$. During these measurements $I_{Ca,L}$ was elicited by 16 consecutive pulses at 0.5 Hz to 0 mV from -80 mV holding potential. The current amplitudes were normalized to the $I_{Ca,L}$ amplitude elicited by the first pulse. Facilitation was not significantly different for $Rem^{-/-}$ (8 + 4%) compared with that in wild-type cardiac myocytes (6 ± 3%; **Fig. S2**).

β-adrenergic stimulation increases Rem blockade of $I_{Ca,L}$ in heterologous expression systems.[16] Also, it is well-established that β-adrenergic stimulation increases the $I_{Ca,L}$ amplitude, and causes a negative shift of $I_{Ca,L}$ activation. Thus, in the absence of Rem, we predict there is a greater dynamic range of $I_{Ca,L}$ responsiveness to β-adrenergic stimulation. To test this hypothesis, we superfused isoproterenol onto cardiomyocytes during the whole-cell recording. The $I_{Ca,L}$ response to isoproterenol was greater for $Rem^{-/-}$ compared with wild-type cardiac myocytes. 10^{-8} M isoproterenol caused a 28 ± 4% and 22 ± 3% increase in $I_{Ca,L}$ amplitude of $Rem^{-/-}$ and wild-type myocytes, respectively. Isoproterenol

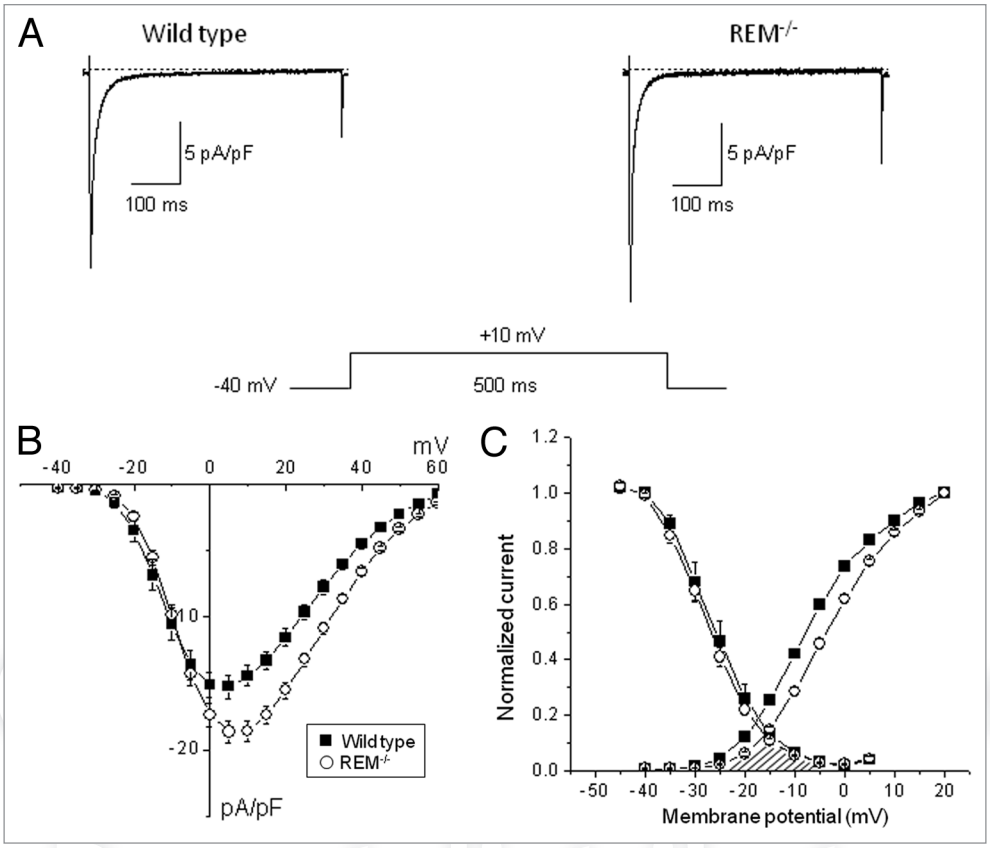

Figure 2. $I_{Ca,L}$ density for wild-type and Rem$^{-/-}$ cardiac ventricular myocytes. (A) Representative original traces from wild-type and Rem$^{-/-}$ mice. (B) Average $I_{Ca,L}$-V relationships for wild-type and Rem$^{-/-}$ cardiac myocytes. (C) The voltage dependence of steady-state activation and steady-state inactivation of $I_{Ca,L}$ for wild-type and Rem$^{-/-}$ cardiac myocytes. $V_{½}$ of steady-state activation is significantly shifted +4 mV for Rem$^{-/-}$ compared with wild type. $V_{½}$ was obtained from fitting the current-voltage data as in (B) to a modified Boltzmann distribution of the form: $I(V) = G_{max} \times (V - E_{rev})/(1 + \exp(V_{½} - V)/k)$, where G_{max} is maximal conductance, E_{rev} is reversal potential, $V_{½}$ is activation midpoint potential and k is the slope factor. The voltage dependence of steady-state inactivation of $I_{Ca,L}$ was measured by a double-pulse protocol. The overlap of steady-state activation and steady-state inactivation curves (cross-hatched) illustrates decrease of window $I_{Ca,L}$ in Rem$^{-/-}$ compared with wild-type cardiac myocytes.

treatment caused no significant shift in the midpoint ($V_{1/2}$) of steady-state inactivation curve. In the presence of 10^{-8} M isoproterenol inactivation $V_{1/2}$ was -29.8 ± 1.0 mV for Rem$^{-/-}$ and -28.9 ± 0.5 mV for wild-type cells. Isoproterenol shifted the voltage dependence of steady-state activation by -6.2 ± 1.0 mV for Rem$^{-/-}$, but only -3.9 ± 1.3 mV for wild type (**Fig. 3**). As a consequence, isoproterenol-modulated channel voltage-dependence was no longer significantly different between Rem$^{-/-}$ and wild type. These data are consistent with the notion that Rem serves as a governor of β-adrenergic stimulated $I_{Ca,L}$.

The Na^+-Ca^{2+} exchange current (I_{NCX}) is the major efflux pathway that homeostatically balances cytosolic Ca-entry via $I_{Ca,L}$.[17,18] The increased peak $I_{Ca,L}$ can be offset by a positive shift of LTCC activation. Therefore, as a surrogate for assessing net trans-sarcolemmal $I_{Ca,L}$ entry we measured I_{NCX}. I_{NCX} was recorded as a Ni^{2+}-sensitive current using the descending limb of a ramp pulse changing from +60 to -100 mV. Outward and inward I_{NCX} were determined at +40 and -80 mV, respectively (**Fig. 4**). Rem$^{-/-}$ have a significantly smaller inward I_{NCX} (0.90 ± 0.16 pA/pF) than for the wild type (1.92 ± 0.4 pA/pF; $p < 0.05$, n = 7; **Fig. 4B**). The mean outward current was larger in wild-type

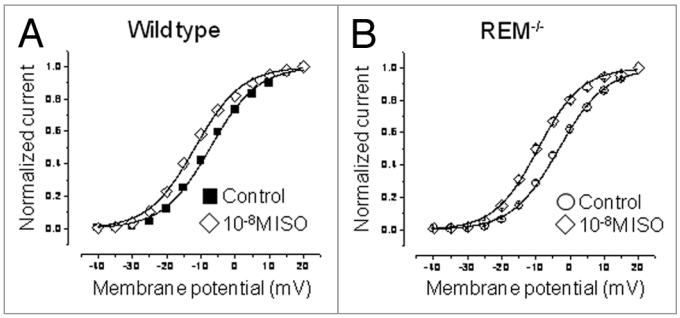

Figure 3. Isoproterenol normalizes the shift of activation $V_{½}$ for Rem$^{-/-}$ compared with wild type. (A) Activation curves for wild-type $I_{Ca,L}$ in control bath and 10 nM isoproterenol ($V_{½}$ for control and isoproterenol were -7.2 ± 0.3 mV and -11.7 ± 0.3 mV, respectively; $p < 10^{-3}$; n = 12). (B) Activation curves for Rem$^{-/-}$ $I_{Ca,L}$ in control bath, and following 10 nM isoproterenol ($V_{½}$ for control and isoproterenol were -3.3 ± 0.2 mV and -9.4 ± 0.3 mV, respectively; $p < 10^{-4}$; n = 24).

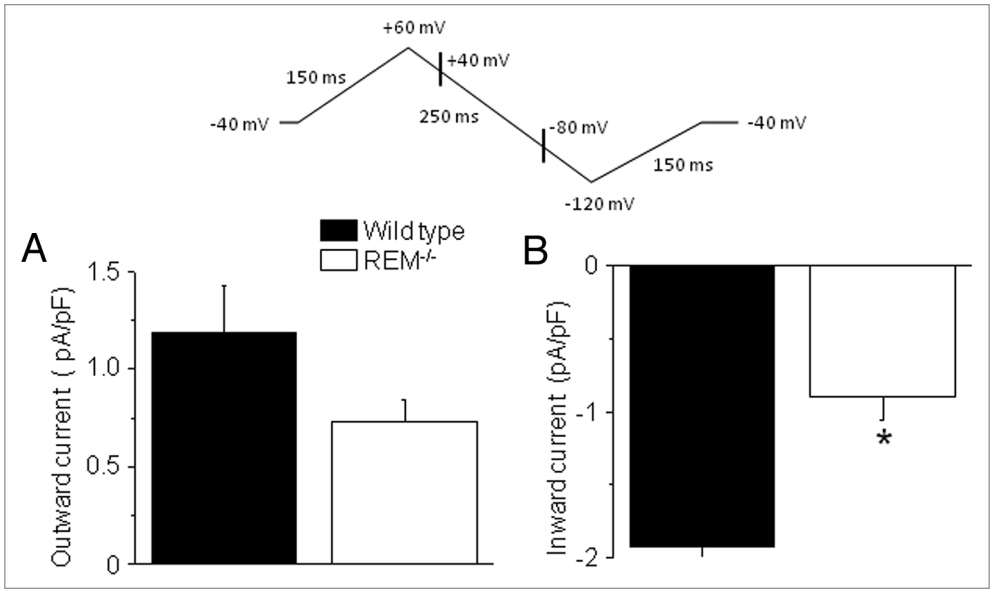

Figure 4. I_{NCX} in wild-type and Rem$^{-/-}$ ventricular myocytes. Upper part shows voltage protocol. Outward I_{NCX} measured at +40 mV, and inward I_{NCX} measured at -80 mV as indicated on hyperpolarizing ramp. Mean I_{NCX} is greater in wild type compared with control for (A) outward and (B) inward current. *p < 0.05.

cells compared with that of Rem$^{-/-}$ cells, but the difference was not significant statistically (1.19 ± 0.24 pA/pF vs. 0.73 ± 0.11 pA/pF for wild-type and for Rem$^{-/-}$ myocytes, respectively, N.S., n = 7; **Fig. 4A**). These results are consistent with the notion that Rem$^{-/-}$ net LTCC trans-sarcolemmal Ca flux may be reduced relative to wild-type cardiac myocytes.

Ca^{2+}-transients and contractility in Rem$^{-/-}$ cardiac myocytes. Despite the increase of maximal peak $I_{Ca,L}$ in Rem$^{-/-}$ cardiomyocytes, the shift of activation, and the decrease of I_{NCX} suggest that in intact cells Rem deletion leads to reduced LTCC function. To determine the impact of Rem deletion on Ca^{2+}-handling, we simultaneously measured whole-cell Ca^{2+} transients and cell shortening (**Fig. 5**). Isolated ventricular myocytes were paced with 1 Hz field stimulation. The amplitude of twitch Ca^{2+} was significantly smaller for Rem$^{-/-}$ compared with wild type (0.35 ± 0.03 vs. 0.27 ± 0.02 for wild-type and for Rem$^{-/-}$ myocytes, respectively, p < 0.01, n = 25 and n = 19 for Rem$^{-/-}$ and wt, respectively; **Fig. 5A and B**). Ten nM isoproterenol significantly increased twitch Ca amplitude in both Rem$^{-/-}$ and wild type, but in the presence of isoproterenol the twitch Ca amplitude remained significantly smaller for Rem$^{-/-}$ relative to wild type.

The decaying phase of Ca transients was fitted to an exponential function to summarize the kinetics of Ca extrusion. The absence of Rem had no effect on the decay time constant (0.14 ± 0.01 sec for Rem$^{-/-}$ and 0.15 ± 0.01 sec, for wild-type cells, N.S., n = 25 and n = 19 for Rem$^{-/-}$ and wt, respectively, **Fig. 5C**). Ten nM isoproterenol did not significantly alter the rate of Ca extrusion. The calcium load of SR was evaluated by a pulse of 5 mM caffeine, which was applied at the end of each experiment. SR Ca^{2+} load was unchanged by Rem knockout (**Fig. 5B**).

In spite of the smaller twitch Ca amplitude fractional cell shortening was not significantly different between Rem$^{-/-}$ and wild type (**Fig. 5D**). Time to peak and relaxation kinetics of cell shortening was faster in Rem$^{-/-}$ compared with wild-type myocytes (**Fig. S3**). The time to peak values of Rem$^{-/-}$ and wild type were 110 ± 4 ms and 132 ± 7 ms (n = 21; p < 0.05), while the half relaxation time was 77 ± 5 ms and 124 ± 16 ms (n = 21; p < 0.05), respectively. 10 nM isoproterenol treatment decreased the time-to-peak values compared with normal pre-drug treatment values in both animal groups (**Fig. S3B**). Isoproterenol treatment reduced the half relaxation time by 20 ± 8 ms in wild-type animals (n = 21; p < 0.05), but we did not observe significant change of this parameter in of Rem$^{-/-}$ (**Fig. S3B**). Cell shortening kinetics is a measure of a complex process. Shortening time reflects Ca-induced Ca release, Ca diffusion and contractile apparatus response. Relaxation kinetics is dominated by cytosolic Ca clearance. Taken together these results suggest that the effect of the chronic absence of Rem extends beyond modulation of $I_{Ca,L}$.

Computer simulations. To explain our results we employed a newly developed computational model of mouse ventricular myocytes.[19] Our approach was to re-adjust LTCC-related parameters based on data from $I_{Ca,L}$ recordings in Rem$^{-/-}$ vs. wild-type myocytes, and then have the model generate Ca^{2+} transients. **Figure 5E** shows the activation and steady-state inactivation curves for $I_{Ca,L}$ superimposed with the model output. The computer simulations quantitatively capture the resulting decrease of 1-Hz stimulated Ca transients (**Fig. 5F**). In addition, the tendency for the mean sarcoplasmic reticulum Ca reduction was also present in the model output. Cell-size adjustments had only modest effects on Ca transients (data not shown). These results are consistent with the contention that a +4 mV shift of LTCC activation results in a decreased Ca-transient, despite a larger maximal conductance.

Compensatory responses. The positive shift of basal $I_{Ca,L}$ activation suggests that $Ca_V1.2$ protein might be less phosphorylated in Rem$^{-/-}$ compared with wild type. The $Ca_V1.2$ distal carboxyl terminus (DCT) Ser1928 is a known substrate for the

β-adrenergic-PKA signaling axis in cardiomyocytes.[20,21] Cardiomyocyte lysates show that DCT migrates at about 37 kDa.[22] The specificity for the antibody used to probe for Ser1928^{P} is demonstrated in **Figure S4**. Fractional DCT-S1928^{P}/total-DCT was significantly less in Rem$^{-/-}$ (51 ± 3%; n = 4) compared with that in wild-type ventricular lysates (78 ± 4%; n = 4; p < 0.002; **Fig. 6A**). We also tested phospholamban (PLB) phosphorylation to assess whether this was a general elevation of PKA signaling. PLB-Ser16 is a PKA substrate site,[23] and there was no difference in PLB-Ser16^{P} between wt and Rem$^{-/-}$ (**Fig. 6B and C**). PLB-Thr17 is an established CaMKII substrate. Although the mean PLB-Thr17^{P} was greater in wt than Rem$^{-/-}$, the differences were not statistically significant (**Fig. 6B and C**).

We postulated that an increase of $I_{Ca,L}$ density in the absence of Rem expression, could in theory, be offset by a compensatory decrease of $Ca_V1.2$ protein expression. To test this straightforward notion, we evaluated immunoblots from isolated ventricular membrane fractions. We observed a significant decrease of full-length $Ca_V1.2$ protein for Rem$^{-/-}$ compared with wild type (74 + 4%; p < 0.01; **Fig. 6D**). The other major RGK protein in the myocardium, Rad, was not different in Rem$^{-/-}$ hearts (**Fig. S5**).

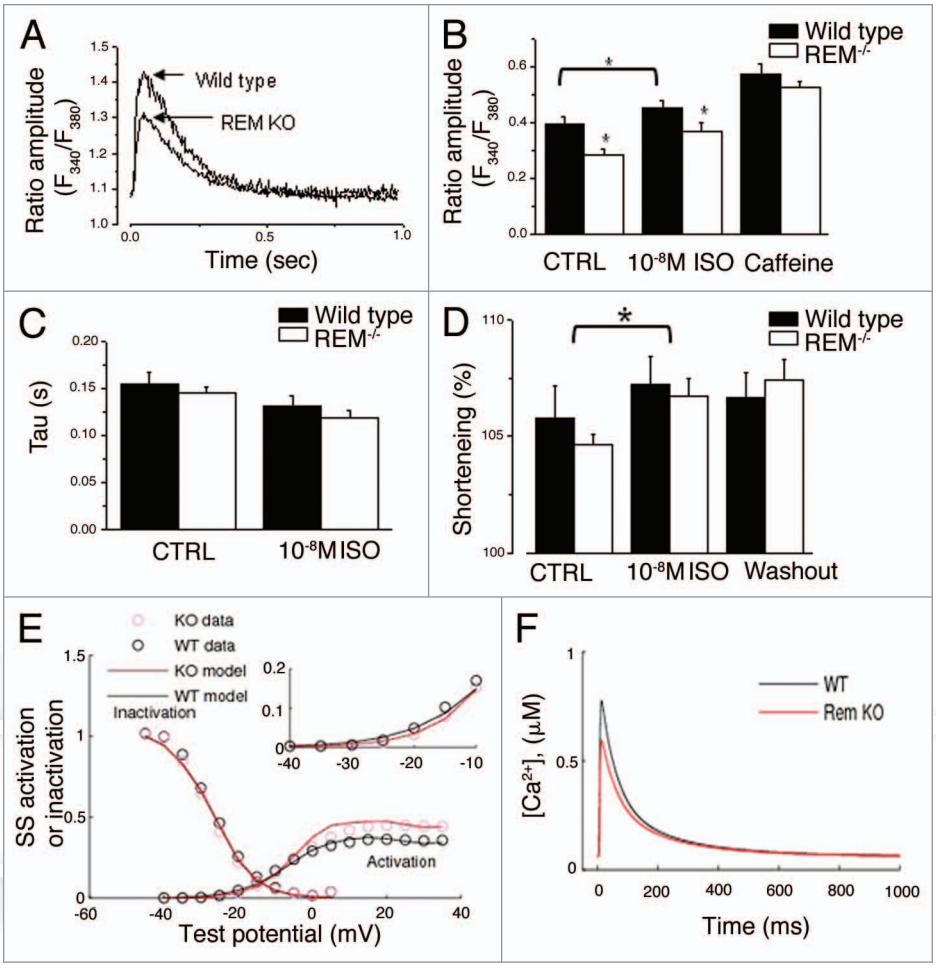

Figure 5. Ca-transients in intact ventricular myocytes. One Hz pacing reveals decreased twitch amplitude, without an effect on SR load in Rem$^{-/-}$ cardiomyocytes. (A) Representative single twitch Ca^{2+}-transient from myocytes 1 paced at 1 Hz. (B) Rem$^{-/-}$ twitch Ca-amplitude is significantly smaller than that in wild type. SR Ca-load was assessed by rapid application of 10 mM caffeine. SR Ca load is not significantly different between Rem$^{-/-}$ and wild type. n = 25 and 19, Rem$^{-/-}$ and wild type, respectively; *p < 0.01 control; *p < 0.05 in isoproterenol. (C) Decay kinetics of twitch Ca transients are not significantly different between Rem$^{-/-}$ and wild type. (D) Simultaneous measure of fractional cell shortening revealed no significant different between Rem$^{-/-}$ and wild type in either control or isoproterenol bath solution. (E and F) Computer simulations capture the decreased Ca transient amplitude in response to a +4 mV shift of $I_{Ca,L}$ steady-state activation. (E) Superimposed steady-state inactivation curve normalized to maximal conductance and steady-state activation curve. For the activation curve, G_{max} = 0.45 pS/pF for Rem$^{-/-}$ and 0.35 pS/pF for wt. Inset shows activation curves expanded for voltage ranging from -40 to -10 mV. (F) Simulated Ca^{2+}-transients shows smaller peak Ca^{2+}-transient amplitude in Rem$^{-/-}$ compared with wt.

Discussion

Overexpressed Rem blocks $I_{Ca,L}$ in myocytes suggesting that endogenous Rem might provide tonic blockade of $I_{Ca,L}$. Thus, eliminating Rem expression was expected to increase $I_{Ca,L}$. The major finding of this study is that Rem knockout results in an increased $I_{Ca,L}$ density. This is the first time that RGK GTPase modification of $I_{Ca,L}$ has been shown following in vivo knockout. Rem deletion also resulted in a depolarizing shift of channel activation, and this shift was normalized to control by β-adrenergic stimulation.

Rem is one of three RGK proteins (Rem, Rad and Gem) expressed by cardiac myocytes. To date, all RGK proteins share the functional property of blockade of $I_{Ca,L}$ when overexpressed in either cardiac myocytes,[4,16] or other cells,[6,14] including those expressing recombinant proteins.[3] In contrast, loss-of-function studies reveal that Rad knockdown via shRNA,[12] or Rad-dominant negative mutant overexpression[24] leads to increased $I_{Ca,L}$ density. A Rad-null mouse has been described in reference 11, but unfortunately no information regarding $I_{Ca,L}$ is available in these studies. At baseline, Rad-null mice have no phenotypic differences from control cardiac myocytes and hearts;[11] however, in view of our present findings it would be reasonable to re-evaluate Rad-null mice. Such a study might shed light on possible non-redundant functions of Rad vs. Rem in cardiac myocytes.

A partial decrease of Rad via shRNA increases $I_{Ca,L}$ and leads to a similar increase of SR Ca-release.[12] The parallels between depressing Rad function and the present report of Rem knockout are partial. Elimination of Rem also increases $I_{Ca,L}$ density, but does not alter SR Ca-load. However, twitch Ca release was

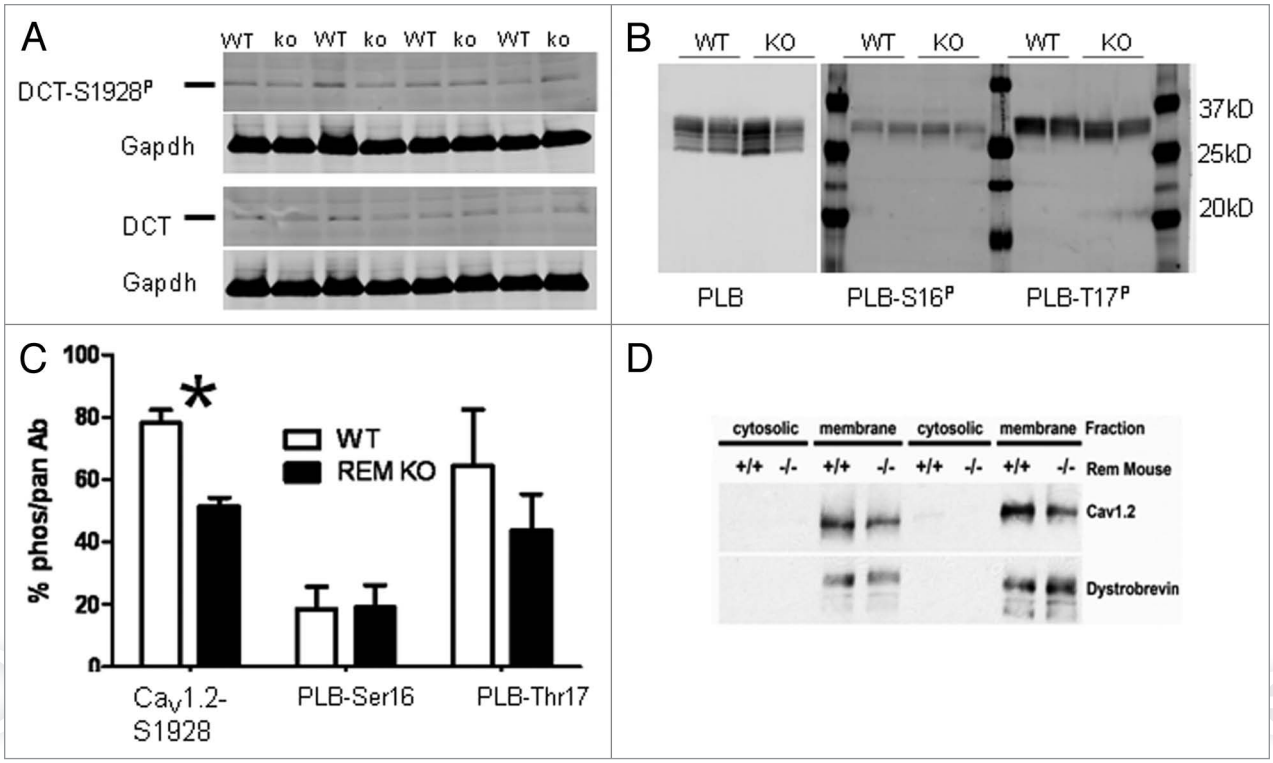

Figure 6. Analysis of $Ca_V1.2$ and phospholamban phosphorylation in wt and $Rem^{-/-}$. (A) Protein extracts from wild-type and $Rem^{-/-}$ hearts were subjected to western blotting and probed with antibodies recognizing $Ca_V1.2$ distal carboxyl terminus (DCT) and DCT-Ser1928^P. Size marker (horizontal line) is 37 kDa. n = 4 $Rem^{-/-}$ and n = 4 wild type. (B) Protein extract was not boiled prior to gel loading to preserve multimeric PLB structure. Six bands for PLN are resolvable; Ser16^P and Thr17^P are confined to upper two bands. (C) Bar graph summarizes fractional phosphorylation. *p < 0.002; n = 4 $Rem^{-/-}$ and n = 4 wild type. PLB phosphorylation was not significantly different. n = 6. (D) $Ca_V1.2$ expression is downregulated in $Rem^{-/-}$ vs. wt heart; 74 ± 4% decrease in $Rem^{-/-}$ vs. wild type; n = 3 $Rem^{-/-}$ and n = 3 wild type; p < 0.01.

diminished. There are at least two non-competing mechanistic interpretations of how Ca-transients can be diminished despite elevated $I_{Ca,L}$ density in $Rem^{-/-}$ cardiac myocytes. Rem may interfere with excitation-contraction coupling directly; alternatively, $I_{Ca,L}$ driven by the action potential may be reduced in $Rem^{-/-}$ cardiac myocytes. Computer simulations support this notion. The +4 mV activation shift is sufficient to decrease $I_{Ca,L}$, despite an elevated maximally-activated conductance, and this activation shift may responsible for the reduced twitch Ca amplitude. Interestingly the reduced twitch Ca amplitude did not cause a change of shortening amplitude. The activation shift in Rem-null cardiac myocytes is consistent with relatively fewer de-phosphorylated LTCC. Elevated $I_{Ca,L}$ leads to cardiac hypertrophy.[25] Thus, it is plausible to view the shift of $I_{Ca,L}$ activation as a compensatory protective effect against increased LTCC G_{max} in the absence of Rem expression.

Other compensatory responses that might occur in $Rem^{-/-}$ mice are more complex. For example, there is an elevated in vivo heart rate (data not shown) consistent with elevated basal sympathetic tone. In this light, the relative de-phosphorylation of $Ca_V1.2$ could protect against Ca-overload via hyper-active $I_{Ca,L}$. However, we could not detect a change in PLB phosphorylation status, despite assessing conditions that preserved pentameric PLB. Note that such conditions show more pronounced changes in the phosphorylation status of Ser16 and Thr17.[26] The difference in relative phosphorylation status of $Ca_V1.2$ and PLB can reside in a number of factors, including but not limited to differential accessibilities to PKA and differential modulation by a variety of phosphatases.

We used $Ca_V1.2$-Ser1928 phosphorylation as a surrogate for the capacity of LTCC to serve as a substrate for PKA activity. The function of $Ca_V1.2$-Ser1928^P is controversial, but the conservation of Ser1928 across species indirectly argues for physiological relevance. Two recent studies argue convincingly that Ser1700^P and Ser1704^P confer β-adrenergic receptor initiated modulation,[21] whereas Ser1928^P is not necessary for $I_{Ca,L}$ modulation.[27,28] Nonetheless, data are also convincing that Ser1928 is a substrate for PKA in cardiac myocytes.[20]

The mechanism for Rem alteration of $I_{Ca,L}$ has been the focus of several recent studies. Early suggestions were that Rem blocks current via 'sponging' $Ca_V\beta$; however, several lines of evidence argue in favor of a model whereby a Rem-LTCC interaction occurs at the cell surface. Despite RGK overexpression, $Ca_V1.2$ can be detected at the cell surface in heterologous expression systems,[13] neurons,[29] and other excitable cells.[13] In addition, Ca^{2+}-channel agonists causes rescue of $I_{Ca,L}$ despite RGK overexpression in cardiac myocytes.[4] Thus, it follows that in the absence of Rem, $Ca_V1.2$ channels at the surface are unmasked. This does not preclude alternative mechanisms of RGK modulation of LTCC function, particularly changes in

stability of LTCC complexes on the plasma membrane whereby Rem promotes $Ca_V1.2$ internalization.[15] We measured less total $Ca_V1.2$ protein concomitantly with more maximally activated $I_{Ca,L}$. This would be consistent with less $Ca_V1.2$ internalization in the absence of Rem expression. Unfortunately we were not able to directly assess endogenous $Ca_V1.2$—this will be an important prediction to evaluate in future studies. To counterbalance higher maximal $I_{Ca,L}$ the activation curve shift prevents excessive Ca^{2+} load as discussed above. It will be interesting to explore additional compensatory mechanisms possibly operating to maintain Ca-homeostasis. In summary our data are consistent with Rem null resulting in increased $I_{Ca,L}$; this is the opposite result to that in response to Rem overexpression in cardiac myocytes.[16]

In conclusion, the major finding of this study is that Rem-null mice display increased $I_{Ca,L}$. The increased $I_{Ca,L}$ density is accompanied by a positive shift of the activation curve resulting in a predicted, yet paradoxical decrease of $I_{Ca,L}$ entry at voltages corresponding to the plateau of the action potential. Thus, Rem modulates $I_{Ca,L}$ in vivo, and cardiac myocytes compensate for modulated $I_{Ca,L}$ to maintain Ca-homeostasis.

Methods

Generation of Rem$^{-/-}$ mice. Mice were housed in a pathogen-free facility and handled in accordance with standard use protocols, animal welfare regulations, and the NIH *Guide for the Care and Use of Laboratory Animals*. All protocols were approved by the University of Kentucky Institutional Animal Care and Use Committee. A targeting vector (**Fig. 1**) containing approximately 11.4 kb of the murine *Rem1* gene was constructed from 129/Sv strain mouse genomic DNA. Additional details are provided in the **Supplemental Methods**.

Adult ventricular myocyte cell isolation, electrophysiology and calcium imaging. Single ventricular myocytes from female mice were enzymatically isolated following a modified AfCS protocol PP00000125 as previously described in reference 30. External Ca was added incrementally back to the solution to 2.0 mM. Only rod-shaped, quiescent myocytes with clear edges were selected for current recording.

Ionic currents were recorded from Ca-tolerant female mouse ventricular cells at 37°C, 1–6 h post-isolation. Currents were recorded with the whole-cell configuration of the patch-clamp technique.

$I_{Ca,L}$ was elicited by 500 ms long depolarizations to various test potentials arising from the holding potential of -40 mV. The stimulation frequency was 0.2 Hz. Peak current amplitude was defined as a difference between the peak value of $I_{Ca,L}$ and its pedestal measured at the end of the pulse. $I_{Ca,L}$ was normalized to cell capacitance.

Na^+/Ca^{2+} exchanger (NCX) current was recorded in voltage-clamped ventricular myocytes as described previously in reference 31. Briefly, NCX current was recorded using ramp pulses (shown in inset to **Fig. 3**). Outward and inward NCX currents were determined during the descending limb of the ramp at +40 and -80 mV, respectively. After taking the control record in K^+-free solution, the cell was superfused with 10 mM $NiCl_2$ in order to fully block the current. Thus, total NCX current was determined at both membrane potentials as a Ni^{2+}-sensitive current.

The measurements of intracellular calcium concentration were done on isolated cardiac myocytes. The cells were loaded with 2 μM fura-2-a.m. for 45 min. All recordings were performed at 20–22°C. Cells were paced for a minimum of 2 min at 1 Hz before recordings to allow steady-state Ca loading. At the end of each measurement, the intracellular calcium store was emptied by a pulse of 5 mM caffeine. During the caffeine pulse the cells were not stimulated. Cell shortening was recorded simultaneously using IonOptix myocam and software.

Additional recording conditions are presented in the **Supplemental Methods**. In all recordings the mouse of origin genotype was encoded to blind the investigator.

Computer simulations. Computer modeling was performed using the framework of the previously developed electrophysiology model for murine ventricular myocytes at 35°C. The difference in cell volume between the wild type and Rem$^{-/-}$ was calculated based on average measurements of the cell surface area and cell length and under the assumption that the myocytes are cylindrical in shape. The volumes of the junctional SR, network SR and dyadic space were adjusted according to their percentages (0.35, 1.05 and 0.1%, respectively) of the myoplasmic volume. The differences in the cell capacitance, myoplasmic volume and the volumes of the intracellular compartments between the wild type and Rem$^{-/-}$ were incorporated into the model during parameterization of the $I_{Ca,L}$.

Parameters for $I_{Ca,L}$ were fitted to experimental measurements obtained from the wild type and Rem$^{-/-}$, including the voltage-dependence of activation and inactivation kinetics, the current-voltage relationship, and the decay kinetics of the current, as described previously in reference 31. All other parameters for the wild-type and the Rem$^{-/-}$ models were unchanged from the existing model.[19]

Western blot analysis. Hearts were excised from wild-type and Rem$^{-/-}$ mice and the left ventricles were isolated. Additional details are in **Supplemental Methods**. Anti-pan phospholamban (PLB) was obtained from Thermo Scientific and S16^P and T17^P-phospholamban antibodies were purchased from Badrilla Ltd. (UK). The $Ca_V1.2$ distal carboxyl terminus (DCT) antibodies (pan-DCT and S1928^P-DCT) custom designed (ECM Biosciences). **Figure S4** shows a representative blot demonstrating phospho-selectivity of the S1928^P-antibody; for these experiments a group of treated cells was exposed to 10 μM forskolin and 30 μM 3-isobutyl-1-methylxanthine (IBMX) for 10 min immediately prior to cell harvest. The Rad antibody was the kind gift of Dr. CR Kahn (Joslin Diabetes Center, Harvard Medical School). The anti-Rem antibody was monoclonal anti-Rem (24E4) from Gamma-One Laboratories. All antibodies were diluted in 5% milk blocking buffer and incubated either over night at 4°C or for at least 1 h at room temperature with rocking. The membranes were washed and incubated with secondary antibody for use on the Li-Cor Odyssey Imaging System and analyzed using their software.

Disclosure of Potential Conflicts of Interest

No potential conflicts of interest were disclosed.

Acknowledgments

We thank Ling Jin for assisting in the generation and maintenance of the Rem$^{-/-}$ mouse colony. Gabriela Hernandez and Douglas Yozwiak provided outstanding technical support.

Sources of Funding

Supported by NIH HL072936 (D.A.A., J.S.), HL07491 (J.S.), 2P20 RR020171 (D.A.A.), OTKA 73,160 (J.M.), MRC G0800980 (N.S.) and Challenge Grant ES018636.

Supplemental Material

Supplemental material may be found here:
http://www.landesbioscience.com/journals/channels/article/20192/

References

1. Dai S, Hall DD, Hell JW. Supramolecular assemblies and localized regulation of voltage-gated ion channels. Physiol Rev 2009; 89:411-52; PMID:19342611; http://dx.doi.org/10.1152/physrev.00029.2007.
2. Benitah JP, Alvarez JL, Gómez AM. L-type Ca(2+) current in ventricular cardiomyocytes. J Mol Cell Cardiol 2010; 48:26-36; PMID:19660468; http://dx.doi.org/10.1016/j.yjmcc.2009.07.026.
3. Finlin BS, Mosley AL, Crump SM, Correll RN, Ozcan S, Satin J, et al. Regulation of L-type Ca^{2+} channel activity and insulin secretion by the Rem2 GTPase. J Biol Chem 2005; 280:41864-71; PMID:15728182; http://dx.doi.org/10.1074/jbc.M414261200.
4. Xu X, Marx SO, Colecraft HM. Molecular mechanisms and selective pharmacological rescue, of Rem-inhibited $Ca_V1.2$ channels in heart. Circ Res 2010; 107:620-30; PMID:20616312; http://dx.doi.org/10.1161/CIRCRESAHA.110.224717.
5. Pang C, Crump SM, Jin L, Correll RN, Finlin BS, Satin J, et al. Rem GTPase interacts with the proximal $Ca_V1.2$ C-terminus and modulates calcium-dependent channel inactivation. Channels (Austin) 2010; 4:192-202; PMID:20458179; http://dx.doi.org/10.4161/chan.4.3.11867.
6. Béguin P, Nagashima K, Gonoi T, Shibasaki T, Takahashi K, Kashima Y, et al. Regulation of Ca^{2+} channel expression at the cell surface by the small G-protein kir/Gem. Nature 2001; 411:701-6; PMID:11395774; http://dx.doi.org/10.1038/35079621.
7. Correll RN, Pang C, Niedowicz DM, Finlin BS, Andres DA. The RGK family of GTP-binding proteins: regulators of voltage-dependent calcium channels and cytoskeleton remodeling. Cell Signal 2008; 20:292-300; PMID:18042346; http://dx.doi.org/10.1016/j.cellsig.2007.10.028.
8. Finlin BS, Andres DA. Rem is a new member of the Rad- and Gem/Kir Ras-related GTP-binding protein family repressed by lipopolysaccharide stimulation. J Biol Chem 1997; 272:21982-8; PMID:9268335; http://dx.doi.org/10.1074/jbc.272.35.21982.
9. Reynet C, Kahn CR. Rad: a member of the Ras family overexpressed in muscle of type II diabetic humans. Science 1993; 262:1441-4; PMID:8248782; http://dx.doi.org/10.1126/science.8248782.
10. Béguin P, Mahalakshmi RN, Nagashima K, Cher DH, Ikeda H, Yamada Y, et al. Nuclear sequestration of beta-subunits by Rad and Rem is controlled by 14-3-3 and calmodulin and reveals a novel mechanism for Ca^{2+} channel regulation. J Mol Biol 2006; 355:34-46; PMID:16298391; http://dx.doi.org/10.1016/j.jmb.2005.10.013.
11. Chang L, Zhang J, Tseng YH, Xie CQ, Ilany J, Brüning JC, et al. Rad GTPase deficiency leads to cardiac hypertrophy. Circulation 2007; 116:2976-83; PMID:18056528; http://dx.doi.org/10.1161/CIRCULATIONAHA.107.707257.
12. Wang G, Zhu X, Xie W, Han P, Li K, Sun Z, et al. Rad as a novel regulator of excitation-contraction coupling and beta-adrenergic signaling in heart. Circ Res 2010; 106:317-27; PMID:19926875; http://dx.doi.org/10.1161/CIRCRESAHA.109.208272.
13. Correll RN, Pang C, Finlin BS, Dailey AM, Satin J, Andres DA. Plasma membrane targeting is essential for Rem-mediated Ca^{2+} channel inhibition. J Biol Chem 2007; 282:28431-40; PMID:17686775; http://dx.doi.org/10.1074/jbc.M706176200.
14. Finlin BS, Crump SM, Satin J, Andres DA. Regulation of voltage-gated calcium channel activity by the Rem and Rad GTPases. Proc Natl Acad Sci USA 2003; 100:14469-74; PMID:14623965; http://dx.doi.org/10.1073/pnas.2437756100.
15. Yang T, Xu X, Kernan T, Wu V, Colecraft HM. Rem, a member of the RGK GTPases, inhibits recombinant $Ca_V1.2$ channels using multiple mechanisms that require distinct conformations of the GTPase. J Physiol 2010; 588:1665-81; PMID:20308247; http://dx.doi.org/10.1113/jphysiol.2010.187203.
16. Crump SM, Correll RN, Schroder EA, Lester WC, Finlin BS, Andres DA, et al. L-type calcium channel alpha-subunit and protein kinase inhibitors modulate Rem-mediated regulation of current. Am J Physiol Heart Circ Physiol 2006; 291:1959-71; PMID:16648185; http://dx.doi.org/10.1152/ajpheart.00956.2005.
17. Lester WC, Schroder EA, Burgess DE, Yozwiak D, Andres DA, Satin J. Steady-state coupling of plasma membrane calcium entry to extrusion revealed by novel L-type calcium channel block. Cell Calcium 2008; 44:353-62; PMID:19230140; http://dx.doi.org/10.1016/j.ceca.2008.01.004.
18. Pott C, Yip M, Goldhaber JI, Philipson KD. Regulation of cardiac L-type Ca^{2+} current in Na^+-Ca^{2+} exchanger knockout mice: functional coupling of the Ca^{2+} channel and the Na^+-Ca^{2+} exchanger. Biophys J 2007; 92:1431-7; PMID:17114214; http://dx.doi.org/10.1529/biophysj.106.091538.
19. Li L, Niederer SA, Idigo W, Zhang YH, Swietach P, Casadei B, et al. A mathematical model of the murine ventricular myocyte: a data-driven biophysically based approach applied to mice overexpressing the canine NCX isoform. Am J Physiol Heart Circ Physiol 2010; 299:1045-63; PMID:20656884; http://dx.doi.org/10.1152/ajpheart.00219.2010.
20. Hulme JT, Westenbroek RE, Scheuer T, Catterall WA. Phosphorylation of serine 1928 in the distal C-terminal domain of cardiac $Ca_V1.2$ channels during β1-adrenergic regulation. Proc Natl Acad Sci USA 2006; 103:16574-9; PMID:17053072; http://dx.doi.org/10.1073/pnas.0607294103.
21. Fuller MD, Emrick MA, Sadilek M, Scheuer T, Catterall WA. Molecular mechanism of calcium channel regulation in the fight-or-flight response. Sci Signal 2010; 3:70; PMID:20876873; http://dx.doi.org/10.1126/scisignal.2001152.
22. Schroder E, Byse M, Satin J. L-type calcium channel C terminus autoregulates transcription. Circ Res 2009; 104:1373-81; PMID:19461046; http://dx.doi.org/10.1161/CIRCRESAHA.108.191387.
23. Colyer J. Phosphorylation states of phospholamban. Ann NY Acad Sci 1998; 853:79-91; PMID:10603938; http://dx.doi.org/10.1111/j.1749-6632.1998.tb08258.x.
24. Yada H, Murata M, Shimoda K, Yuasa S, Kawaguchi H, Ieda M, et al. Dominant negative suppression of Rad leads to QT prolongation and causes ventricular arrhythmias via modulation of L-type Ca^{2+} channels in the heart. Circ Res 2007; 101:69-77; PMID:17525370; http://dx.doi.org/10.1161/CIRCRESAHA.106.146399.
25. Nakayama H, Chen X, Baines CP, Klevitsky R, Zhang X, Zhang H, et al. Ca^{2+}- and mitochondrial-dependent cardiomyocyte necrosis as a primary mediator of heart failure. J Clin Invest 2007; 117:2431-44; PMID:17694179; http://dx.doi.org/10.1172/JCI31060.
26. Sachan N, Dey A, Rotter D, Grinsfelder DB, Battiprolu PK, Sikder D, et al. Sustained hemodynamic stress disrupts normal circadian rhythms in calcineurin-dependent signaling and protein phosphorylation in the heart. Circ Res 2011; 108:437-45; PMID:21233454; http://dx.doi.org/10.1161/CIRCRESAHA.110.235309.
27. Ganesan AN, Maack C, Johns DC, Sidor A, O'Rourke B. Beta-adrenergic stimulation of L-type Ca^{2+} channels in cardiac myocytes requires the distal carboxyl terminus of alpha1C but not serine 1928. Circ Res 2006; 98:11-8; PMID:16397147; http://dx.doi.org/10.1161/01.RES.0000202692.23001.e2.
28. Lemke T, Welling A, Christel CJ, Blaich A, Bernhard D, Lenhardt P, et al. Unchanged beta-adrenergic stimulation of cardiac L-type calcium channels in $Ca_V1.2$ phosphorylation site S1928A mutant mice. J Biol Chem 2008; 283:34738-44; PMID:18829456; http://dx.doi.org/10.1074/jbc.M804981200.
29. Chen H, Puhl HL, 3rd, Niu SL, Mitchell DC, Ikeda SR. Expression of Rem2, an RGK family small GTPase, reduces N-type calcium current without affecting channel surface density. J Neurosci 2005; 25:9762-72; PMID:16237180; http://dx.doi.org/10.1523/JNEUROSCI.3111-05.2005.
30. Schroder E, Magyar J, Burgess D, Andres D, Satin J. Chronic verapamil treatment remodels $I_{Ca,L}$ in mouse ventricle. Am J Physiol Heart Circ Physiol 2007; 292:1906-16; PMID:17158651; http://dx.doi.org/10.1152/ajpheart.00793.2006.
31. Birinyi P, Acsai K, Bányász T, Tóth A, Horváth B, Virág L, et al. Effects of SEA0400 and KB-R7943 on Na^+/Ca^{2+} exchange current and L-type Ca^{2+} current in canine ventricular cardiomyocytes. Naunyn Schmiedebergs Arch Pharmacol 2005; 372:63-70; PMID:16086157; http://dx.doi.org/10.1007/s00210-005-1079-x.